

A study of patch antenna arrays on alumina substrate

G. N. PASCARIU*, O. G. AVĂDĂNEI, S. B. BALMUS^a, I. DUMITRU, P. GASNER

Faculty of Physics, "Al. I. Cuza" University of IASI, Romania

^aScience Department, "Al. I. Cuza" University of IASI, Romania

The rapid development of the communication infrastructure in the last time, has imposed a constant research effort in developing of new materials, microsystems and microstructures which would aloud a greater degree of miniaturization, and a better stability with temperature. The main requirement for miniaturization of the components is a high value of the dielectric permittivity of the material. It is also necessary a low dielectric loss to assure a better efficiency of the device in our case of the patch antenna, and o good stability with the temperature to assure a better frequency stability of the antenna or array.

(Received August 3, 2010; accepted October 14, 2010)

Keywords: Microstrip antenna arrays, Dielectric permittivity, Phase excitation, Pattern radiation

1. Introduction

The paper concerns the study of patch antennas with alumina (Al₂O₃) dielectric substrate. Compactness of microstrip antennas has made them very attractive for applications in communication systems. As the need for antenna miniaturization continues, a possible solution is offered by utilization of alumina dielectric materials as substrate.

The frequency dependence of alumina permittivity (both real and imaginary parts) and patch antenna resonance and radiation characteristics are presented and discussed.

Very interesting are the microstrip antenna array configurations. The number of elements is imposed by the feeding system of the array, which must provides the same phase for all the patches.

We discuss also a comparative study between two possibilities: all elements in phase or elements are of different phases. In fact, antenna arrays can be designed to control their radiation characteristics by properly selecting the phase and/or amplitude distribution between array elements. Antenna patterns for some circular arrays with different phase excitations are presented.

2. Models and main relations for a single microstrip patch antenna and antenna arrays

For the characterization of the microstrip antenna proprieties we take into account the cavity model and for the its excitation we use the transmission line model. The basic relations refer to the radiation patterns of patches and to the input impedances. The rectangular patch and the coordinate system for the cavity model are shown in Fig. 1. In order to establish some important relations concerning the radiation pattern of a patch a simple model was adopted: the field \vec{E} has only z component whereas the field \vec{H} has only x y components; both \vec{E} and \vec{H} are

independent of z coordinate for all the frequencies of interest; the tangent component of the \vec{H} along the edge has a negligible value, therefore the electric current has no component perpendicular to the edge. This simple model can be applied for patch antennas because they have a very small dimension along the z axe.

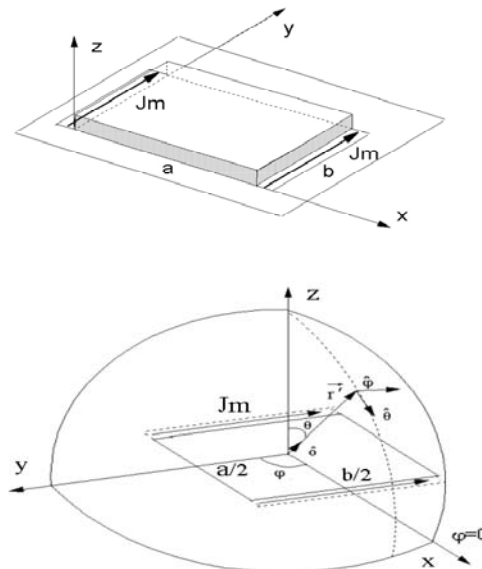


Fig. 1. The rectangular microstrip patch and it's coordinates system.

The region between patch and ground plane can be treated as a cavity bounded by magnetic walls along the edge and by electric walls on the top and bottom. If such a cavity is excited by a microstrip line or by a coaxial line Fig. 2 the field inside cavity represent a superposition of all TM_{mno} modes; the z component of \vec{E} can be assumed as [1], [2]:

$$E_z(x, y) = \sum_m \sum_n A_{mn} \bar{e}_{mn}(x, y) \quad (1)$$

where A_{mn} are the mode amplitude coefficient and \bar{e}_{mn} are the z -directed orthonormalized electric field mode vector.

For a nonradiating cavity the E_z component has the following form:

$$E_z = E_0 \cos k_m x \cos k_n y \cos k_p z \quad (2)$$

and the x, y components of magnetic fields are:

$$\begin{aligned} H_x &= \frac{j\omega_r \epsilon}{k_{mnp}^2} k_y E_0 \cos k_m x \sin k_n y \cos k_p z \\ H_y &= \frac{j\omega_r \epsilon}{k_{mnp}^2} k_x E_0 \sin k_m x \cos k_n y \cos k_p z \end{aligned} \quad (3)$$

where: $k_{mnp}^2 = k_m^2 + k_n^2 + k_p^2$, and $k_m = m\pi/a$ $k_n = n\pi/b$ $k_p = p\pi/t$; ω_r is the resonant frequency.

Usually a dominant mode of oscillation is assumed; such a mode is TM_{100} described by the relations:

$$E_z = E_0 \cos \pi x / a \quad (4)$$

$$H_y = jH_0 \sin \pi x / a \quad (5)$$

where $H_0 = E_0/Z$ and $Z = (\mu_0 / \epsilon_r)^{1/2}$.

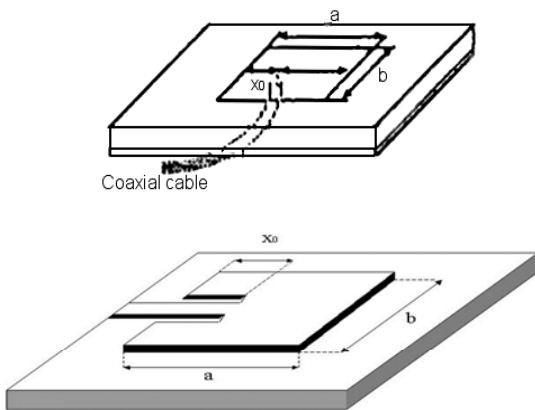


Fig. 2. Coaxial feed patch and microstrip line feed patch.

In the case of radiating microstrip patches (real cavity) the eigenvalues became complex quantities and $|k_m|, |k_n|$ are slightly less than $m\pi/a$ and $n\pi/b$.

For the dominant mode TM_{100} we have only magnetic currents on the edge, defined by general relation

$\vec{J}_{ms} = -\hat{n} \times \vec{E}_a$ where \vec{E}_a is the electric field in the aperture at the edge and \hat{n} is the outgoing unit vector from the edge.

It is shown that only the currents [1]:

$$\begin{aligned} \vec{J}_{ms1}(x=0) &= -2\hat{n} \times \vec{E}_a = \hat{j}2E_z(x, y) \\ \vec{J}_{ms2}(x=a) &= -2\hat{n} \times \vec{E}_a = \hat{j}2E_z(x, y) \end{aligned} \quad (6)$$

are radiating in the free space.

In order to analyze the radiating properties of the microstrip patch antennas we will assume the coordinate system shown in Fig. 1, in which the coordinate origin coincides with the symmetry center of the antenna. The radiated fields in the Fraunhofer zone have the expressions [7]:

$$\begin{aligned} E_\theta &= -\frac{jk}{\pi r} \exp(-jk_0 r) E_0 \cdot \int_{-b/2}^{b/2} \int_{-a/2}^{a/2} e^{j(k_0 y \sin \theta \sin \phi)} \left(e^{-\frac{jk_0 a \sin \theta \cos \phi}{2}} + e^{\frac{jk_0 a \sin \theta \cos \phi}{2}} \right) dy dx \cos \phi \\ E_\phi &= -\frac{jk}{\pi r} \exp(-jk_0 r) E_0 \cdot \int_{-b/2}^{b/2} \int_{-a/2}^{a/2} e^{j(k_0 y \sin \theta \sin \phi)} \left(e^{-\frac{jk_0 a \sin \theta \cos \phi}{2}} + e^{\frac{jk_0 a \sin \theta \cos \phi}{2}} \right) dy dx \sin \phi \cos \theta \end{aligned} \quad (7)$$

From these relations we can determine the radiated fields until a constant E_0 that depends of the excitation.

The input impedance of a patch antenna is of great practical importance because if the patch is not adapted to the feed line the antenna would not radiate at all. The input impedance is calculated by the relation [1],[2]:

$$\frac{1}{R_{mn}} = \frac{\mu_0 h c^2}{\epsilon_r \omega_{mn} \delta_{eff}} \psi_{mn}^2(x_0, y_0) G_{mn} \quad (8)$$

where $G_{mn} = \frac{\sin(n\pi d_x / 2a)}{n\pi d_x / 2a} \cdot \frac{\sin(m\pi d_y / 2b)}{m\pi d_y / 2b}$

and $\psi_{mn} = \frac{\chi_{mn}}{\sqrt{ab}} \cos k_n x \cos k_m y$

The factor G_{mn} accounts for the width of the feed, c is the speed of light, δ_{eff} is an effective loss tangent in which are included also the losses in metallic walls and the radiating losses, and χ_{mn} is a normalization factor. For microstrip feed patch antennas the effective feed dimensions (d_x, d_y) are taken equal to the physical dimensions of the microstrip line.

The radiation pattern for array antennas is found by multiplying the array factor with the radiating pattern of one element. The array factor for planar array with m elements on x -coordinate and n elements on y -coordinate is given by [2], [7]:

$$E = E_0 \sum_{s=1}^m \exp(j(s-1)(\delta + kdx \sin \theta \cos \varphi)) \cdot \sum_{s=1}^n \exp(j(s-1)(\delta + kdy \sin \theta \sin \varphi)) \quad (9)$$

where δ is the phase factor between two consecutive elements and dx , dy are the distances between two consecutive elements along the x respective y axes; E_0 is the field radiated by a single patch.

3. Experimental and simulations results

3.1. Studied antennas

We have designed, using 1.2 mm thick white and 1 mm thick pink alumina (Al_2O_3) substrates, two patch antennas for 2.8 GHz which are presented in Fig. 3.

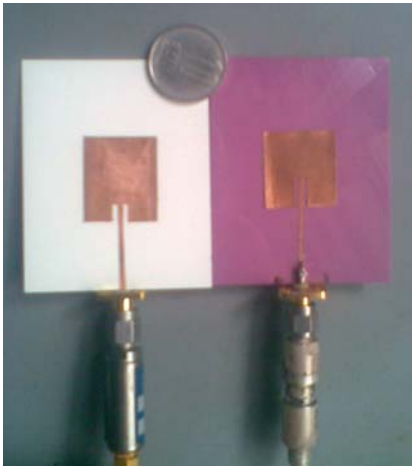


Fig. 3. Studied microstrip antennas.

The patches dimensions obtained from the calculus, using the cavity model, are: 19 mm \times 20 mm for the white alumina antenna and 19 mm \times 22 mm for the pink alumina antenna.

3.2. Permittivity measurements

In order to obtain correct results in the antenna characteristics simulations the permittivity of the alumina substrate must be exactly measured.

Using an AGILENT E8361A Network Analyzer the permittivity - frequency dependencies in the microwave range for the white and pink alumina used for our antennas were obtained and they are presented in Fig. 4 and Fig. 5.

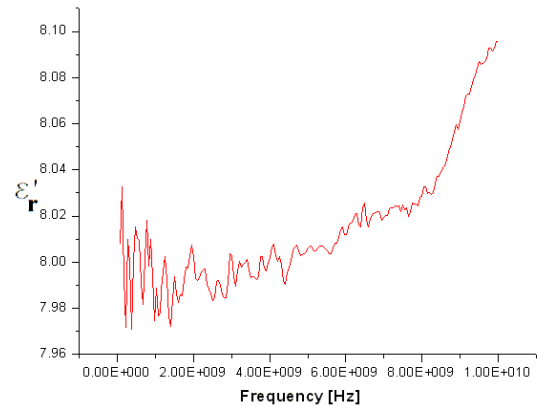


Fig. 4. The permittivity - frequency dependence for the white alumina.

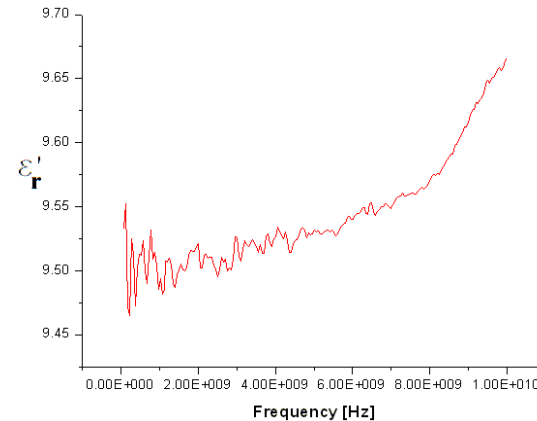


Fig. 5. The permittivity - frequency dependence for the pink alumina.

The white alumina dielectric substrate is characterized by the real permittivity $\epsilon_r' = 7.98 \div 8.01$ between 2 GHz and 4GHz and the pink alumina dielectric substrate is characterized by the real permittivity $\epsilon_r' = 9.48 \div 9.53$ between 2 GHz and 4GHz.

For designing our antenna with a 2.8 GHz resonance frequency we considered for the white alumina substrate $\epsilon_r' = 8$ and for the pink alumina substrate $\epsilon_r' = 9.5$.

3.3. Resonance frequencies

After designing and building the two antennas, their resonance characteristics were measured using the same AGILENT E8361A Network Analyzer and they are presented in Figs. 6 and 7.

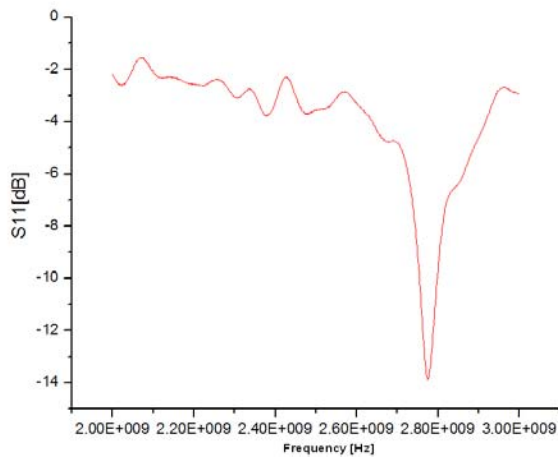


Fig. 6. S_{11} – frequency dependence for the white alumina antenna.

The measured resonance frequency of the white alumina antenna is 2.77 GHz and the measured resonance frequency of the pink alumina antenna is 2.76 GHz, which means that that cavity model used for designing the two antennas is a very suitable model for characterizing the patch antennas.

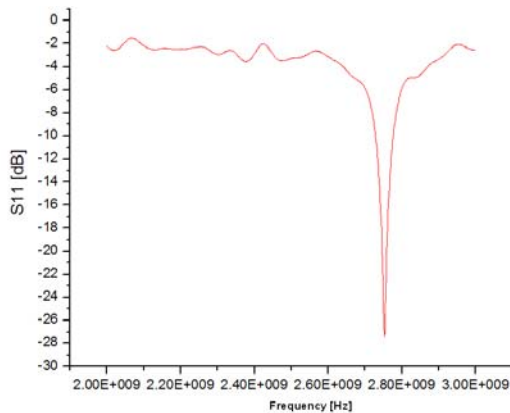


Fig. 7. S_{11} – frequency dependence for the pink alumina antenna.

3.4. Radiation patterns of a single patch antenna

In this section we present simulations regarding the radiation patterns and the dependence of the input impedance with feeding point of the microstrip antennas

The antennas were excited using a coaxial line characterized by an impedance of 50 ohms. For an optimal power transfer between the coaxial line and the microstrip antenna, the input impedance of the antenna, which is strongly dependent of the feeding point, x_0 from Fig. 2, (the distance between the point were the central conductor of the coaxial line is attached to the patch and the corresponding side of the patch), must be the same with the impedance of the coaxial feeding line. In Fig. 8 is presented the dependence of the input impedance with feeding point of the white alumina microstrip antenna.

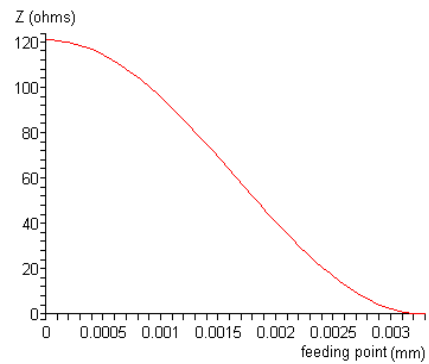


Fig. 8. The Input impedance – feeding point dependence.

In Fig. 9 and 10 are presented the power radiation pattern of the microstrip patch antenna with white alumina substrate in cross section in the far field (Franhofer zone) the microstrip patch antenna and also the three-dimensional antenna pattern of the same antenna.

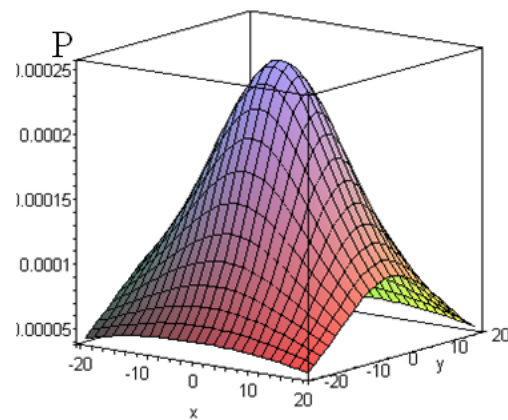


Fig. 9. The power radiation pattern in (x, y) plane in the far field (Franhofer zone) for one patch antenna.

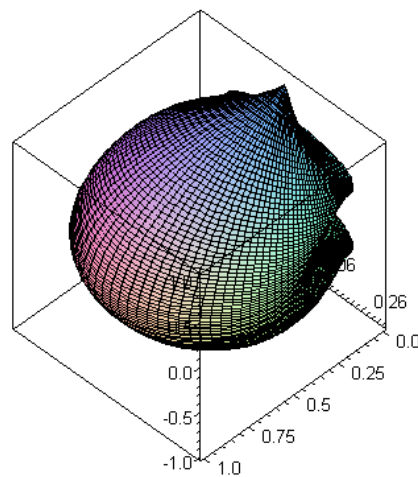


Fig. 10. The three-dimensional radiation pattern of the microstrip antenna with white alumina substrate.

3.5. Patch antenna arrays

3.5.1. Radiation patterns of patch antenna arrays in phase excitation

In this section we present simulations regarding the characteristics and the radiation patterns of some patch antenna planar circular arrays.

In Fig. 11 are presented the spherical coordinate system used for our simulation calculus and also the points where are placed the patch antennas indexed from 1 to N.

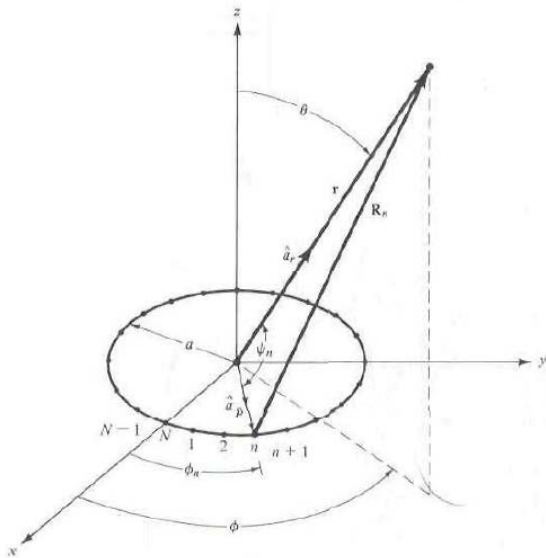


Fig. 11. The spherical coordinate system and the patch antennas placement points.

Initially we considered that all the patch antennas of the arrays are feed in phase and that they are independent, the influences between antennas are considered negligible.

In Fig. 12 is presented in cross section the radiation pattern of a patch antenna circular array (9 cm radius) with 12 elements

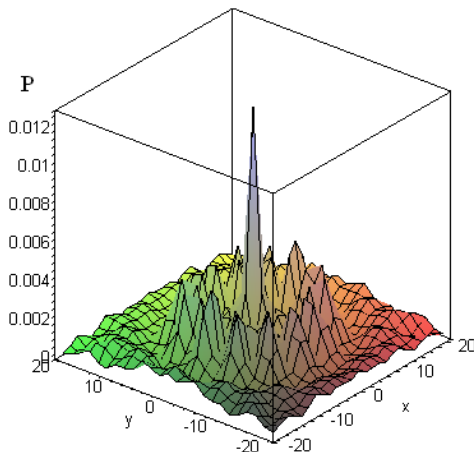


Fig. 12. The radiation pattern in cross section of a patch antenna circular array (9 cm radius) with 12 elements.

We can observe a principal lobe above the center of the circular array and 12 secondary smaller lobes above the centers of each patch antenna.

In Fig. 13 is presented in cross section the radiation pattern of a patch antenna circular array (9 cm radius) with 15 elements

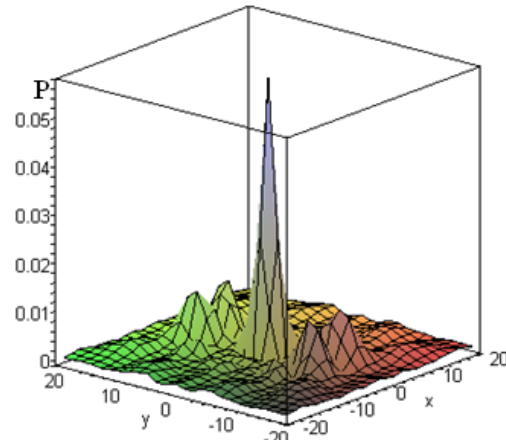


Fig. 13. The radiation pattern in cross section of a patch antenna circular array (9 cm radius) with 15 elements.

We can observe that the principal lobe above the center of the circular array increases and that the lobes above the centers of each patch antenna interfere and create other secondary lobes which are not situated above the centers on the patch antennas.

The total radiation field, emitted by a specifically array of patch antennas, was calculated by multiplying the field emitted by a single antenna with the factor array [3], [4], [7].

$$E_{total} = E \cdot \sum_{n=1}^N e^{jkr_1 \sin \theta \cos(\phi - \phi_n)} \quad (10)$$

$$E_{total} = EA_t \quad (11)$$

$$A_t = \sum_{n=1}^N e^{jkr_1 \sin \theta \cos(\phi - \phi_n)} \quad (12)$$

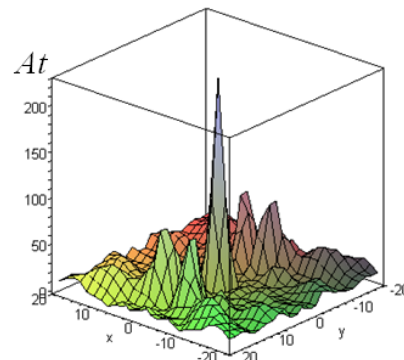


Fig. 14. The factor array in cross section of a patch antenna circular array (9 cm radius) with 15 elements.

3.5.2. Radiation patterns of patch antenna arrays in progressive phase excitation. radiation angle control

In this section are presented simulation results regarding the control of the radiation characteristics (radiation angle) of the patch antenna arrays depending on the feeding mode. In Figs. 15 and 16 are presented the two-dimensional radiation patterns of a patch antenna planar circular array with 7 elements excited in phase

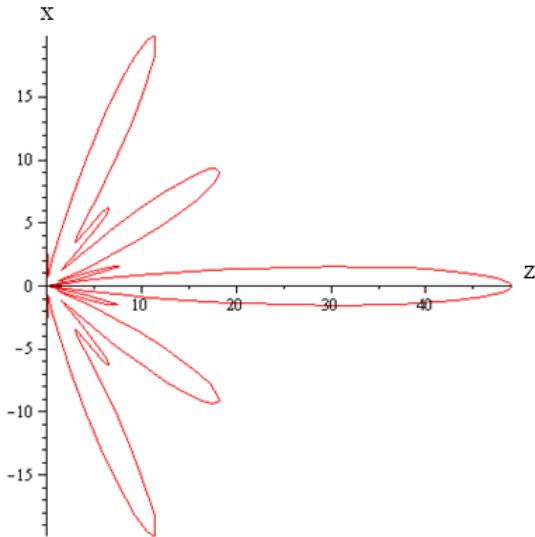


Fig. 15. Antenna pattern in cross section ($\varphi = 0$) of a planar array with 7 patch elements in phase excitation.

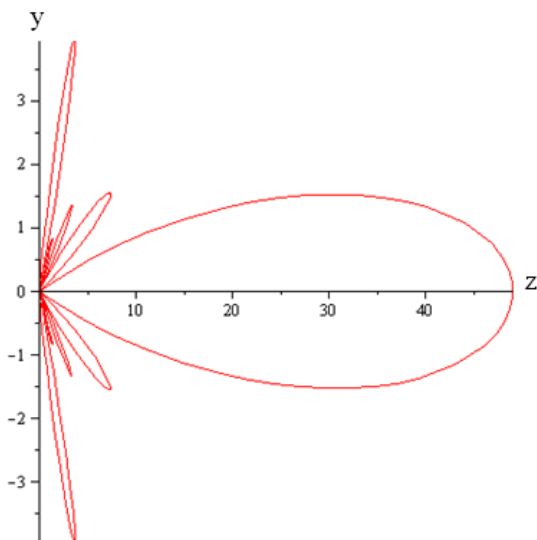


Fig. 16. Antenna pattern in cross section ($\varphi = \pi/2$) of a planar array with 7 patch elements in phase excitation.

In Fig. 17 is presented the three-dimensional antenna pattern of a planar array of 7 patch elements with alumina substrate in phase excitation.

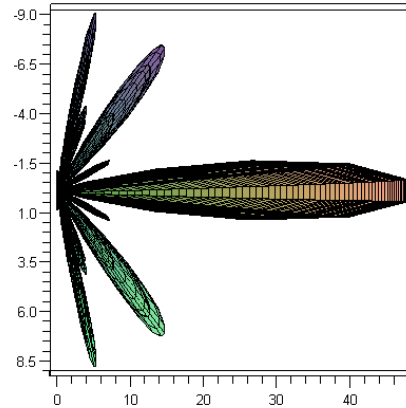


Fig. 17. Three-dimensional antenna pattern of a planar array of 7 patch elements with alumina substrate in phase excitation.

Next we present simulations which show that, by progressive phase feeding the elements of the array, the radiation angle of the principal lobe can be modified. This is called electronically ablation.

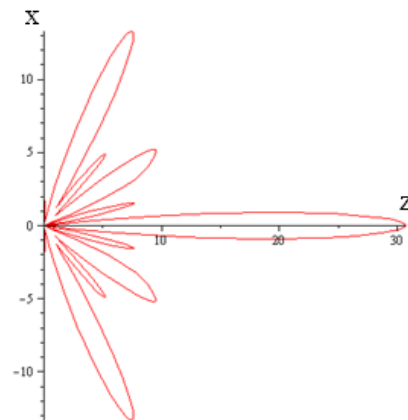


Fig. 18. Antenna pattern in cross section ($\varphi = 0$) of a planar array with 7 patch elements in progressive phase excitation.

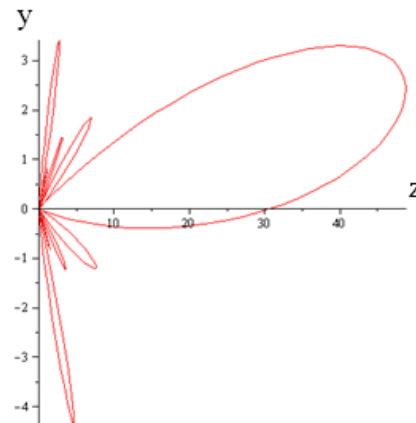


Fig. 19. Antenna pattern in cross section ($\varphi = \pi/2$) of a planar array with 7 patch elements in progressive phase excitation.

In Figs. 18 and 19 are presented the two-dimensional radiation patterns of a patch antenna planar circular array with 7 elements excited in progressive phase.

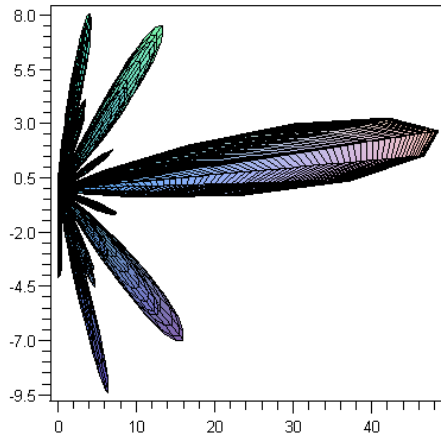


Fig. 20. Three-dimensional antenna pattern of a planar array of 7 patch elements with alumina substrate in progressive phase excitation.

In Fig. 19 and 20 it is shown that, by progressive phase excitation, the radiation angle and the directivity of the patch antenna arrays could be modified, which makes possible the electronically beam steering.

4. Conclusions

The calculated resonance frequencies and the measured resonance frequencies are in good concordance which means that cavity model used for designing the two antennas is a very suitable model for characterizing the patch antennas.

The antenna patterns obtained in our simulations are in good concordance with the ones presented in the literature [5-8].

Antenna array can be designed to control their radiation characteristics by properly selecting the phase and/or amplitude distribution between elements. We studied microstrip rectangular patches array applied on planar surface with alumina substrate.

Low-profile, low-cost antennas support the operation of many modern communication systems. Microstrip patch antennas represent one family of compact antennas that offers the benefits of a conformal nature and the capability of ready integration with a communication system printed circuitry.

Acknowledgements

This work was performed by the following financial supports: Project POSDRU/89/1.5/S/49944 and PN-2 Project PMCDRASSI 12-078.

References

- [1] D. D. Sandu, O. G. Avădănei, A. Ioachim, G. Banciu, P. Gasner, *J. Optoelectron. Adv. Mater.* **5**(5), 1381 (2003).
- [2] O. G. Avădănei, D. D. Sandu, D. Ionesi, *Proc. SCS (IEEE Chapter)*, 37 (2001).
- [3] R. W. P. King, *IEEE Trans. A. P.*, **12**, pg. 269 (1964).
- [4] C. T. Tai, *IEEE Trans. A. P.*, **12**, 447 (1964).
- [5] R. W. P. King, *IEEE Trans. A. P.*, **12**, 276 (1964).
- [6] H. Bach, J. E. Hansen, "Uniformly Spaced Array" in *Antenna Theory* editors R. E. Collin, F. J. Zucker, McGraw-Hill 1969.
- [7] N. Balanis "Antenna theory: Analysis and design", sec. edition, John Wiley&Sons, N.Y. 1997, chapter 6.
- [8] W. W. Hansen, J. R. Woodyard, "A New Principle in Directional Antenna Design" *Proc. IRE*, **26**, 333 (1938).

*Corresponding author: george.pascariu@uaic.ro